

Structure and local order in Co magnetic thin films on Au(111): A surface EXAFS study

N. Marsot

Laboratoire pour l'Utilisation du Rayonnement Electromagnétique (LURE), Bâtiment 209d, Centre Universitaire Paris Sud, 91405 Orsay Cedex, France
and Service de Recherche sur les surfaces et l'Irradiation de la Matière, Commissariat à l'Energie Atomique Saclay, 91191, Gif-sur-Yvette, France

R. Belkhou

Laboratoire pour l'Utilisation du Rayonnement Electromagnétique (LURE), Bâtiment 209d, Centre Universitaire Paris Sud, 91405 Orsay Cedex, France

H. Magnan

Laboratoire pour l'Utilisation du Rayonnement Electromagnétique (LURE), Bâtiment 209d, Centre Universitaire Paris Sud, 91405 Orsay Cedex, France
and Service de Recherche sur les Surfaces et l'Irradiation de la Matière, Commissariat à l'Energie Atomique Saclay, 91191, Gif-sur-Yvette, France

P. Le Fèvre

Laboratoire pour l'Utilisation du Rayonnement Electromagnétique (LURE), Bâtiment 209d, Centre Universitaire Paris Sud, 91405 Orsay Cedex, France

C. Guillot

Laboratoire pour l'Utilisation du Rayonnement Electromagnétique (LURE), Bâtiment 209d, Centre Universitaire Paris Sud, 91405 Orsay Cedex, France
and Service de Recherche sur les Surfaces et l'Irradiation de la Matière, Commissariat à l'Energie Atomique Saclay, 91191, Gif-sur-Yvette, France

D. Chandesris

Laboratoire pour l'Utilisation du Rayonnement Electromagnétique (LURE), Bâtiment 209d, Centre Universitaire Paris Sud, 91405 Orsay Cedex, France
 (Received 4 March 1998)

The structure of cobalt thin films on an Au(111) surface has been studied using x-ray absorption spectroscopy at the cobalt *K* edge. The polarization dependence of x-ray absorption near-edge spectra and extended x-ray absorption fine structure (EXAFS) spectra evidences a hexagonal stacking for films thicker than 4 ML. For all the thicknesses, the analysis of the first-nearest-neighbor shell shows that this hexagonal structure is very close to that of the Co hcp bulk one: the cobalt does not grow in a coherent epitaxy on the Au(111) surface. This incoherent epitaxy leads to a wide radial distribution of the Co-Au bonds at the interface: this effect and the contribution of Au atoms to the EXAFS signal are discussed. The weak strains inside the Co magnetic thin films allow us to neglect the contribution of the magnetoelastic anisotropy to the perpendicular-magnetic anisotropy existing in this system. [S0163-1829(99)00703-1]

I. INTRODUCTION

During the past decade, many studies have been dedicated to ultrathin-film magnetism. Since the theoretical prediction of a strong perpendicular magnetic anisotropy in ultrathin films,¹ several binary systems (ferromagnetic, paramagnetic) have been studied. Among them, the Co-Au system is of particular interest. As a matter of fact, it displays all the original magnetic properties recently observed in bidimensional systems: Co-Au multilayers² show giant magnetoresistance³ and oscillatory behavior of interlayer magnetic coupling.⁴ Thin Co films on Au(111),⁵ as well as sandwiches,⁶ present a perpendicular magnetic anisotropy.⁷ In these thin films, the switching of the magnetization from

out-of-plane to inplane occurs at a critical thickness between 14 and 19 Å.^{5,6} This thickness dependence results from a competition between the surface and bulk contributions⁸ to the total-magnetic anisotropy of the Co layers. Among the different anisotropy contributions proposed, the magneto-crystalline anisotropy depends strongly on the crystallographic and structural parameters of the magnetic films. It is also true for the magnetoelastic contribution, introduced by Chappert and Bruno,⁹ which takes into account the strain effects in the ferromagnetic film due to the lattice mismatch (14% for Co/Au).

The disparity of substrates (textured Au surface, Au single crystal, etc.) in all the previous studies confirms the importance of the knowledge of the film morphology. Thus,

Speckmann, Oepen and Ibach¹⁰ and Jansen *et al.*¹¹ have shown that the magnetic domain's sizes are larger by one order of magnitude in the case of Co films deposited on an Au(111) single crystal, than in films evaporated on Au(111) textured substrates: the substrate roughness and the resulting Co film morphology change the magnetic properties of the sample. Relations between magnetism and morphology are here clearly pointed out, therefore, an explanation of the magnetic behavior of the films requires a precise knowledge of the Co structure (growth mode, interdiffusion, relaxation, etc.).

Only a few studies have been devoted to the characterization of the Co growth mode on the Au(111) single crystal at room temperature (RT). It is now well established that at RT the growth mode is mainly driven by the Au(111) reconstruction.^{12,13} In a previous paper using core-level photoemission spectroscopy,¹⁴ we have described the different stages of the Co growth on Au(111) surface: below 2 ML deposited at RT, the Au surface is essentially covered by bilayer islands. The coalescence of the islands starts above 2 ML and is completed around 3.5 ML. We have also pointed out the presence of an interdiffusion at RT, directly correlated to the Co islands coalescence. The studies of the structure of Co films deposited on fcc substrate, have shown that the Co layers can assume either the fcc structure [Co/Cu(001) (Refs. 15 and 16)] or the hcp one [Co/Cu(111) (Ref. 17)]. On a fcc (111) surface, depending on the stacking period of the hexagonal planes, the cobalt structure can be either a hcp, a fcc or a twinned fcc one (two fcc single domains twinned by 60°). A previous low-energy electron diffraction (LEED) study¹⁴ has shown for Co films a pattern with a sixfold symmetry. So, it is possible to conclude partially between the three possibilities of Co stacking: it is either hcp or twinned fcc. Nevertheless, there is little information about the local order in Co thin films deposited on an Au(111) single crystal. The question of the Co stacking is still open: is it a hcp or a twinned fcc stacking? What is the strain induced by the Au substrate inside the Co thin film? Do the Co layers relax? The aim of this paper is to answer these questions. We have studied the structure of Co thin films on an Au(111) surface using x-ray absorption spectroscopy at the Co K edge, a technique that is sensible to the local order in the Co films. After a description of the experimental procedure, we will present and discuss the results obtained from XANES (x-ray absorption near-edge structure) and surface EXAFS (extended x-ray absorption fine structure) spectra.

II. EXPERIMENTS

The experiments were performed at the "Laboratoire pour l'Utilisation de Rayonnement Electromagnétique" (LURE, France) on the surface EXAFS setup using a Si(311) double-crystal monochromator installed on the wiggler beam line of the DCI storage ring. The Co films are deposited at RT in ultrahigh vacuum (base pressure in the chamber is better than 10^{-10} torr). Repeated cycles of Ar⁺ sputtering and annealing at 900 K lead to well-defined ($\sim 22 \times \sqrt{3}$) reconstruction of the Au(111) surface.¹⁸⁻²⁰ The Co evaporation

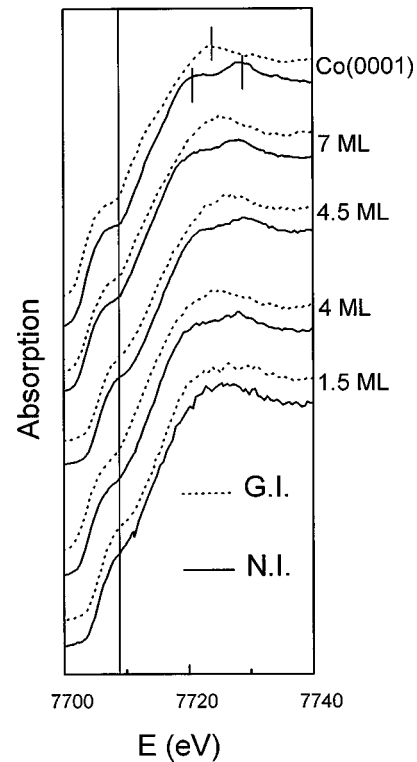


FIG. 1. XANES spectra recorded at 300 K at the Co K edge for different Co films deposited at RT on Au(111) in the NI (solid line) and in the GI (dashed line). The straight line shows the Co threshold (7709 eV).

rate is controlled with a quartz microbalance and thicknesses are checked using auger electron spectroscopy.

We have studied Co films of thicknesses from 1 to 7 ML, deposited at RT on the Au(111) surface. The variations of the x-ray absorption coefficient of the samples are recorded *in situ* at 77 K above the cobalt K edge (7709 eV) in the fluorescence-yield mode. To measure a possible crystallographic anisotropy of the Co films, we have taken advantage of the linear polarization of the x-rays. For each sample two spectra have been recorded: one with a normal incidence (NI) of the x-ray beam (polarization of the x ray in the film plane) and the other in grazing incidence (GI) (polarization is about 70° out of the surface plane). The polarization dependence of the spectra will allow us to measure the first nearest-neighbor distance in the hexagonal planes and out of these planes. It will also provide information on the Co stacking period.¹⁷

III. XANES RESULTS

XANES spectra are very sensitive to the local order around the excited atom. Figure 1 shows the evolution of the Co XANES spectra in the film as a function of Co thickness up to 7 ML. They are compared with reference spectra recorded on a Co(0001) single crystal. For the fcc structure, XANES spectra are not dependent on the x-ray polarization due to the isotropic electric-dipole absorption cross section in a cubic symmetry (O_h). In the hcp structure (full-point group D_{6h}), absorption spectra exhibit an anisotropy due to a dichroic dependence of the electric-dipole K edge absorption

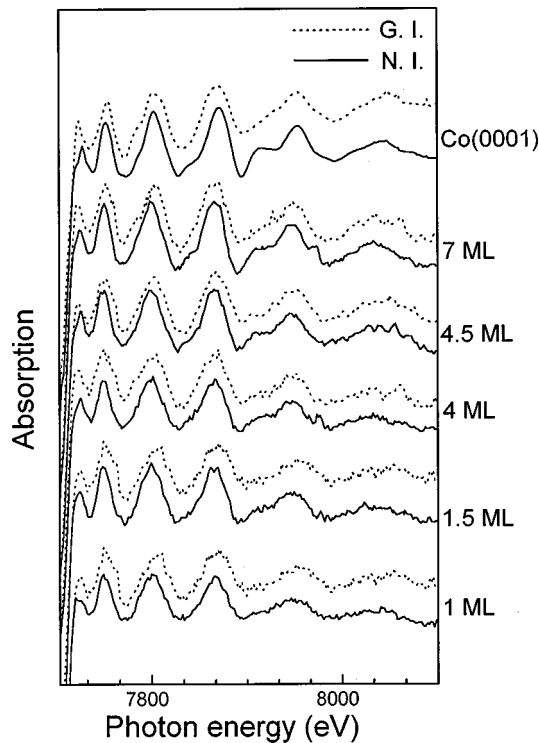


FIG. 2. EXAFS raw spectra recorded at 77 K at the Co K edge for different Co films deposited at RT on Au(111) substrate in NI (solid line) and in GI (dashed line). Spectra recorded at RT on a Co(0001) single crystal are presented too.

cross section:²¹ for Co(0001), the XANES spectra present one bump in GI, and two bumps in NI.¹⁷

From our results it is clear that the thin Co/Au(111) films have a preferential hcp stacking for thicknesses above 4 ML. This trend is not clearly defined for the 1 and the 1.5 ML Co thin films. For these low thicknesses, speaking about hcp or fcc stacking does not make any sense: the quantity of deposited Co does not allow us to complete an ABA or ABC stacking on the Au surface. Nevertheless, it seems that the Co thin film of 1.5 ML presents rather isotropic XANES spectra with one single bump, while for an fcc environment, the spectra should show two bumps for both incidences. This may be attributed to a disordered interface and will be discussed later.

IV. EXAFS RESULTS

More quantitative information was obtained from EXAFS measurements. Figure 2 shows the variations of the x-ray absorption coefficient for different Co/Au(111) films together with spectra recorded on a reference Co(0001) hcp sample. The EXAFS oscillations are well defined even for very low thicknesses (1 and 1.5 ML) both in NI and GI. From the angular dependence of the spectra, one can measure a possible distortion of the Co unit cell.

The angular dependence of the single-scattering part of the EXAFS signal is $\cos^2 \alpha$,²² where α is the angle between the atomic bond and the polarization vector of the x-ray. As shown previously by LEED, on the Au(111) surface Co can have a twinned fcc or a hcp structure. In these two structures, each Co atom has six nearest neighbors (NN) in its plane,

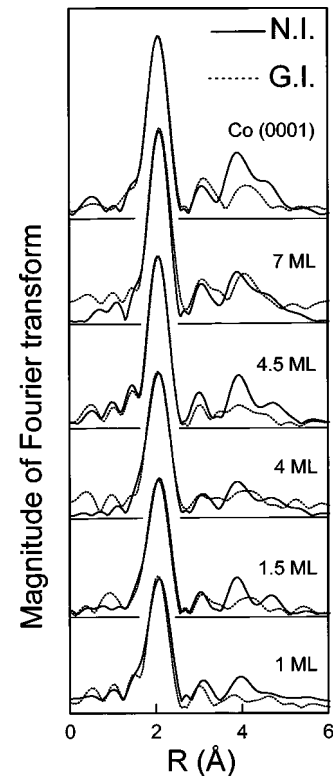


FIG. 3. Fourier transform of $k\chi(k)$, from $k=2.5$ to 11.3 \AA^{-1} , for EXAFS spectra recorded at 77 K in NI (solid line) and in GI (dashed line) of different films of Co/Au(111). For comparison, a FT of a Co(0001) single crystal at RT on the same k window is given too.

three above (missing for the top layer) and three below (Au neighbors for the bottom layer). For the first NN shell, in GI only the bonds with direction out of the (111) planes contribute to the signal (interlayer bonds), while in NI the bonds parallel to the (111) planes (intralayer bonds) have a weight three times larger than the interlayer bonds.

The main frequency of the EXAFS oscillations is the NN distance. One can see in Fig. 2 a polarization dependence of the raw EXAFS spectra: the main frequency is slightly higher in NI than in GI for films thinner than 4 ML. It denotes intralayer bonds lengths larger than the interlayer ones for thin films and increasing interlayer bond length with increasing thickness. However, in all cases, the main frequency of the EXAFS oscillations remains similar to that of Co reference spectra both in GI and NI.

For a quantitative analysis, we have calculated the Fourier transform (FT) of the EXAFS spectra. The first peak of the FT is the contribution of the first NN shell, which can be analyzed with the single-scattering formalism. The other peaks contain both the single-scattering contribution of the more distant neighbor shells, and the multiple-scattering contribution of the NN shell: they can only be modeled in a multiple-scattering formalism.

First, the EXAFS measurements confirm the conclusions drawn from the XANES spectra on the structure of the Co films. On an Au(111) surface, we have seen that the cobalt stacking is either a hcp or a twinned fcc. The EXAFS technique being a very local probe, a twinned fcc structure cannot be distinguished from a fcc one. But, the EXAFS spectra

TABLE I. Results of the least-squares fits of the EXAFS signal of the first shell of neighbors for different Co thicknesses on the Au (111) surface, compared with the values determined for a Co (0001) single crystal. The parameter set is as follows: R the first nearest-neighbor distance, N^* the effective coordination number, and ΔC_2 the relative mean-square displacement.

Co thickness ($\pm 10\%$)	Incidence		N^* (± 1)	R (\AA) (± 0.01)	$\Delta C_2 \times 10^{-3}$ (\AA^2) ($\pm 0.5 \times 10^{-3}$)
Co (0001)	GI	In-plane	0		
		Out-of-plane	12	2.49	
	NI	In-plane	9	2.50	
		Out-of-plane	3	2.49	
7 ML	GI	In-plane	0		
		Out-of-plane	10.3	2.51	1.9
	NI	In-plane	9	2.51	2.5
4.5 ML	GI	Out-of-plane	2.1	2.51	1.9
		In-plane	0		
	NI	In-plane	9	2.50	4.0
4 ML	GI	Out-of-plane	1.6	2.49	1.8
		In-plane	0		
	NI	In-plane	9	2.51	5.1
1.5 ML	GI	Out-of-plane	1.5	2.49	3.0
		In-plane	0		
	NI	In-plane	9	2.52	6.1
1 ML	GI	Out-of-plane	1.5	2.48	0.3
		In-plane	0		
	NI	In-plane	9	2.50	8.4
		Out-of-plane	1.5	2.48	0.8

will be very different for fcc or hcp stacking. In a fcc environment, the first and fourth neighbors are aligned in the (111) plane, and out of this plane, leading to a ‘‘focusing effect’’ both in NI and GI.²³ In a hcp stacking, these alignments exist only in the hexagonal (0001) planes. A strong polarization dependence is then expected for the fourth peak (contribution of the fourth neighbors) in hcp Co FT. Figure 3 shows the evolution of the FT of the EXAFS oscillations as a function of the Co thickness. The R scale is the relative NN distance to within the phase-shift factor. By comparison with the Co(0001) hcp FT, it appears that for Co thicknesses above 4 ML, the different peaks of the FT are at the same positions as in the Co(0001) reference, both in GI and in NI. This result confirms the hcp structure of these films in agreement with XANES observations. The hcp stacking may favor a strong perpendicular-magnetic anisotropy since the (0001) direction is the easy magnetization axis in the hcp bulk Co.²⁴ As for the XANES spectra, no conclusion can be drawn about the stacking of very thin films.

The contribution of the NN shell to the EXAFS signal is calculated by an inverse Fourier transform of the first peak of the FT. This contribution is then fitted using the classical EXAFS formula.^{22,25} The experimental Co backscattering amplitude and phase shifts are extracted from a bulk Co sample EXAFS spectrum. Due to the polarization dependence of the EXAFS oscillations, the number of NN arising in the fit is an effective coordination number N^*

$= 3 \sum_i \cos^2 \alpha_i$, where α_i is the angle between the polarization vector of the x rays and the direction of the bond i .^{16,22} Thus, as pointed out above, only interlayer NN bonds contribute to the GI spectra. For each sample, we have first fitted the GI spectrum to get this interlayer NN distance. Using this value, we have fitted the NI spectrum and deduced the intralayer NN distance. These distances are obtained with an associated mean-square relative-displacement factor σ^2 , giving the width of the radial-distribution function RDF of the first NN shell parallel and perpendicular to the interface. For the fitting procedure and for the 1 and 1.5 ML samples, N^* was calculated assuming large bilayer islands and neglecting the Au NN contribution. For the larger Co coverages, we have also neglected the Au NN contribution, and N^* was fixed to the theoretical values for a flat film (layer-by-layer growth). These assumptions will be discussed in the next section. The results of the fits are presented on Table I: For all thicknesses, the intralayer NN distance is the same as in bulk cobalt ($2.51 \pm 0.01 \text{\AA}$). We can conclude that the cobalt does not grow pseudomorphically on the Au substrate: the Co in-plane NN distance (2.51\AA) is too different from the Au one (2.88\AA). The Co does not grow in coherent epitaxy,²⁶ because of the presence of the reconstruction pattern of the Au(111) surface and/or the large lattice mismatch of 14% between Au and Co. Concerning the interlayer NN distance, it slightly increases with thickness (less than 1%), but it is

still close to that in bulk cobalt (2.49 Å).

The classical EXAFS formula shows a dependence of $\exp(-2k^2\sigma_i^2)$, where k is the photoelectron wave vector and σ_i^2 the mean-square relative displacement between the absorbing atom and the i neighbor. In fact, σ_i contains two contributions, one (σ_{DW}) represents the thermal disorder (Debye-Waller factor) and the other (C_2) the static disorder. C_2 is the width of the RDF. With the fitting procedure, one obtains ΔC_2 the difference between the width of the RDF in the Co films and the one in the Co bulk reference. The resulting ΔC_2 are given in Table I for the different studied Co films. For all thicknesses, the in-plane ΔC_2 factor values are larger than the out-of-plane ones, denoting a larger disorder parallel to the interface. The larger disorder in the plane for very thin films can be explained by the incommensurability between the two-dimensional (2D) lattices of hcp Co and fcc Au. Nevertheless, the evolution of the in-plane ΔC_2 factor values with the Co coverage shows a Co film more and more ordered parallel to the interface. At 7 ML, the order in the film parallel and perpendicular to the interface is the same.

V. THE Co/Au INTERFACE

For the 1 and 1.5 ML samples, we have fitted the data assuming that the Co film was formed by large bilayer islands as previously observed,^{12,14} and neglecting the Au NN. In the GI spectrum recorded for 1 ML Co/Au(111), a single layer should imply only Au effective NN for each Co atom. In this case, the first peak of the FT should present a double structure, due to the complex Au phase shifts.^{27,28} This is clearly not observed in our experiment, showing that the Co layer is at least a bilayer. This is in agreement with the bilayer growth mode observed by the scanning tunnel microscope (STM). Nevertheless, in the case of a bilayer film, one third of the effective NN should be Au atoms. We do not observe any contribution from these Au atoms. We will now explain that this is caused by the disorder at the interface.

First, let us demonstrate that the contribution of the Au atoms can be neglected. A convincing test must be done on the 1 ML GI spectrum, where the interface contribution is the largest. Different fits of the NN contribution extracted from this spectrum are presented in Fig. 4. The variable fitting parameters are the ΔC_2 factor, the first NN distance, and the effective coordination number N^* : fit 1 is done assuming only Au NN at 2.69 Å (single Co layer), using the Au backscattering amplitude and Co-Au phase shifts calculated with the FEFF code;²⁹ fit 2 is done assuming Co large bilayer

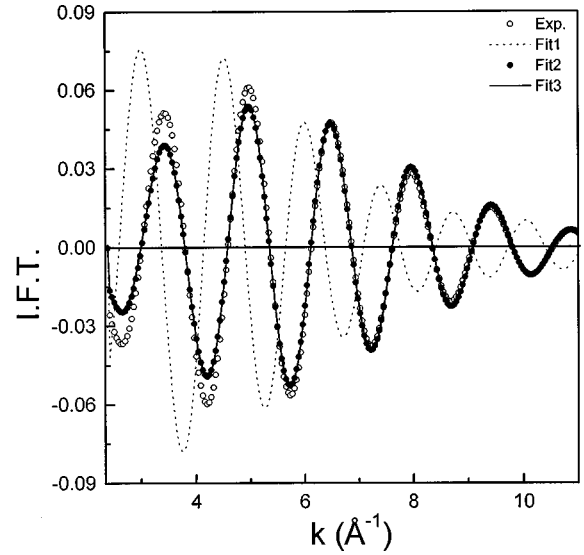


FIG. 4. Comparison between the experimental inverse Fourier transform (IFT) for 1 ML of Co deposited at RT, in grazing incidence and the IFT fits corresponding to three particular cases: fit 1 is done assuming only Au neighbors (6 NN at 2.69 Å, with a ΔC_2 of 0.001 Å²), fit 2 assuming only Co neighbors (6 NN at 2.48 Å, with a ΔC_2 of 0.0008 Å²), and fit 3 taking into account both types of neighbors, i.e., 6 Co NN at 2.48 Å, with a ΔC_2 of 0.0008 Å² and 1.5 Au NN at 2.69 Å, with a ΔC_2 of 0.093 Å².

islands, neglecting Au NN; and fit 3 is done in the same configuration as fit 2, taking into account the Au NN at the Co-Au interface.

The results of the three fits are given in Table II. The first fit clearly does not reproduce our experimental data: it shows that the EXAFS signal cannot be simulated with only Au NN, confirming that the thin film is not a single layer. Fits 2 and 3 reproduce well the experimental data. They give the same interlayer Co NN distance and associated ΔC_2 factor, showing that these parameters can be safely determined, neglecting the presence of Au NN (as it was done in Table I).

On the other hand, the fits of the NN shell contributions demonstrate that a Co(0001) lattice grows incoherently on the Au(111) substrate. The sketch of the two lattices is plotted in Fig. 5(a) [Au(111) bulk plane and Co(0001) plane]. This sketch is used as a model to calculate the intralayer RDF. It clearly shows that the distribution of NN distances between Co and Au atoms is very wide. The incoherent epitaxy may also imply an undulation of the interplanar dis-

TABLE II. Results of the different fits corresponding to the 1 ML Co spectrum in GI. The fits are done assuming these three situations: fit 1 with only Au NN, fit 2 with only Co NN and fit 3 with both Co NN and Au NN. The parameter set is as follows: R the first nearest neighbor distance, N^* the effective coordination number, and ΔC_2 the relative mean-square displacement.

	Au NN			Co NN		
	N^* (± 1)	$R_{\text{Au-Co}}$ (Å) (± 0.01)	$\Delta C_2 \times 10^{-3}$ (Å ²) ($\pm 0.5 \times 10^{-3}$)	N^* (± 1)	$R_{\text{Co-Co}}$ (Å) (± 0.01)	$\Delta C_2 \times 10^{-3}$ (Å ²) ($\pm 0.5 \times 10^{-3}$)
Fit 1	6	2.69	1.0			
Fit 2				6	2.48	0.8
Fit 3	1.5	2.69	93	6	2.48	0.8

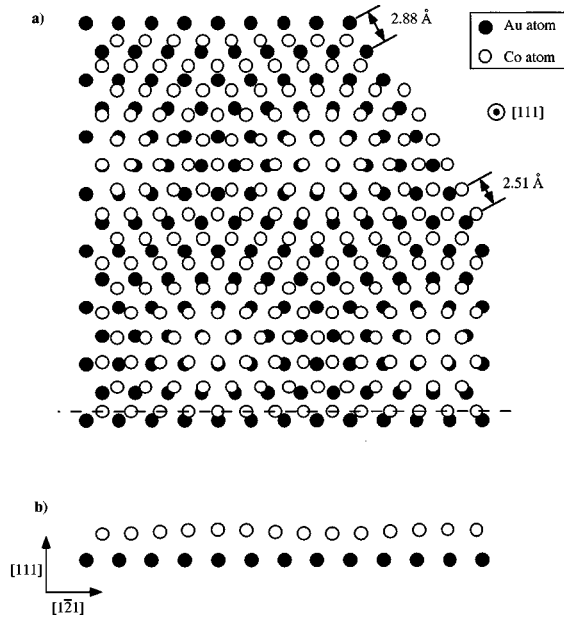


FIG. 5. Sketch of a Co(0001) plane (first neighbors at 2.51 Å) and an Au(111) bulk plane (first neighbors at 2.88 Å), used as a model to calculate the intralayer RDF: (a) top view, (b) side view of the sketch cut along the dashed line.

tance between the Co film and the Au substrate [see Fig. 5(b)], as it has been shown in the case of Co/Pt(111) (Ref. 30) and Co/Pd(111).³¹ Using this scheme, we have calculated the Co-Au RDF assuming an undulation with an average interplanar distance of 2.52 Å (Fig. 6). This distribution can be decomposed in three wide Gaussian functions between 2 and 5 Å: the first Gaussian function corresponds to an average of 1 Au NN at 2.81 Å, with a ΔC_2 factor (width of the RDF) of 0.05Å^2 . This corresponds to a smaller number of intralayer NN, than for a perfectly epitaxied flat layer (3 NN) and to a very damped EXAFS signal (large ΔC_2 factor). Let us note that the Co-Au RDF parameters found in fit 3 are close to the calculated ones. Calculations based on the same scheme as above, but excluding the undulation of the interplanar distance between the Co film and the substrate, have also been done. The results of these calculations are similar to the previous ones (small number of Au NN and large associated ΔC_2 factor).

This section justifies our fitting procedure where Au contribution was always neglected.

Our conclusions on the Co film structure are different from those obtained in the literature.^{3,5} The authors claimed that the epitaxial Co films are strained of 14% for 1 ML and of 8% for 3 ML. According to them, the Co structure is relaxed above 6 ML. However, as the Co/Au critical thickness for a pseudomorphic growth is small⁷ compared to the thickness of the Co bilayer islands, the Co film can never be pseudomorphic even for low coverage. The 14% strain for 1 ML Co claimed by the authors are then highly improbable.

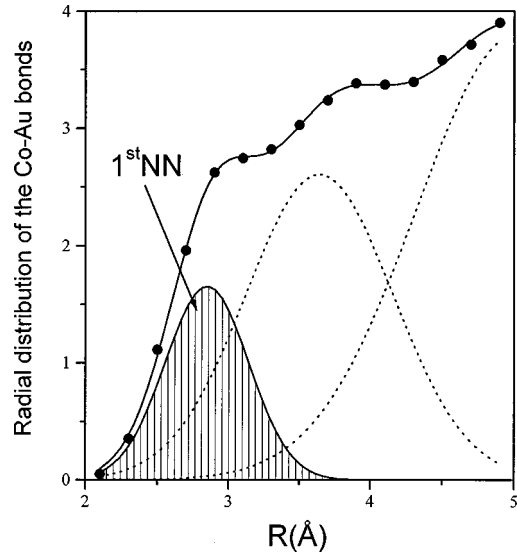


FIG. 6. Radial distribution of the Co-Au interlayer bond as a function of the distance $R(\text{Å})$ between a Co atom and an Au neighbor one, calculated according to the sketch on Fig. 5.

The incoherent epitaxy of the cobalt precisely characterized by EXAFS, is probably due to the weak interaction at the interface between Co and Au atoms and to the large misfit (14%), which is beyond the elastic limits. Concerning the magnetic properties of the Co films and particularly the origin of the perpendicular magnetic anisotropy, we have shown that the magnetoelastic anisotropy cannot contribute to it. A precise magnetic characterization should provide information on the role of the other contributions to the magnetic anisotropy.

VI. CONCLUSION

We have measured the variations of the x-ray absorption coefficient at the cobalt K edge at 77 K for Co films of different thicknesses deposited at room temperature on the Au(111) reconstructed surface. We have shown using XANES and surface EXAFS that the stacking of the cobalt films for thicknesses above 4 ML is hcp, and that the Co does not grow pseudomorphically on the Au(111) surface: there is an incoherent epitaxy, probably caused by the important lattice mismatch between Co and Au (14%), and the presence of the Au(111) reconstruction. The Co $\langle 0001 \rangle$ axis is perpendicular to the Au(111) surface. A consequence of the incoherent epitaxy for the Co-Au interface is a wide-radial distribution of the Co-Au bonds, which leads to a weak contribution to EXAFS signal. Concerning the magnetic properties of the Co/Au(111) system, we have pointed out the Co grown with its own lattice parameter on the Au(111) single crystal. Therefore, any magnetoelastic anisotropy contribution to the perpendicular magnetic anisotropy can be neglected.

- ¹J. G. Gay and R. Richter, Phys. Rev. Lett. **56**, 2728 (1986).
- ²C. H. Lee, H. He, F. Lamelas, W. Vavra, C. Uher, and R. Clarke, Phys. Rev. Lett. **62**, 653 (1989).
- ³C. Dupas, P. Beauvillain, C. Chappert, J. P. Renard, F. Trigui, P. Veillet, E. Vélú, and D. Renaud, J. Appl. Phys. **67**, 5680 (1990).
- ⁴W. B. Zeper, F. J. A. M. Greindamus, P. F. Garcia, and C. R. Fincher, J. Appl. Phys. **65**, 4971 (1989).
- ⁵R. Allenspach, M. Stamparoni, and A. Bischof, Phys. Rev. Lett. **65**, 3344 (1990).
- ⁶J. Pommier, P. Meyer, G. Penissard, P. Bruno, F. Ferre, and D. Renard, Phys. Rev. Lett. **65**, 2054 (1990).
- ⁷C. Chappert and P. Bruno, J. Appl. Phys. **64**, 5736 (1988).
- ⁸T. Kingetsu and K. Sakai, Phys. Rev. B **48**, 4140 (1993).
- ⁹C. Chappert and P. Bruno, Appl. Phys. A: Solids Surf. **49**, 499 (1989).
- ¹⁰M. Speckmann, H. P. Oepen, and H. Ibach, Phys. Rev. Lett. **75**, 2035 (1995).
- ¹¹R. Jansen, M. Speckmann, H. P. Oepen, and H. van Kempen, J. Magn. Magn. Mater. **165**, 258 (1997).
- ¹²B. Voigtlander, G. Meyer, and N. M. Amer, Phys. Rev. B **44**, 10 354 (1991).
- ¹³C. Tolkes, P. Zeppenfeld, M. A. Krzyzowski, R. David, and G. Comsa, Phys. Rev. B **55**, 13 932 (1997).
- ¹⁴N. Marsot, R. Belkhou, F. Scheurer, B. Bartenlian, N. Barrett, and C. Guillot, Surf. Sci. **377–379**, 225 (1997).
- ¹⁵A. Clarke, G. Jennings, R. F. Willis, J. P. Rous, and J. B. Pendry, Surf. Sci. **187**, 327 (1987).
- ¹⁶O. Heckmann, H. Magnan, P. Le Fèvre, D. Chandris, and J. J. Rehr, Surf. Sci. **312**, 62 (1994).
- ¹⁷P. Le Fèvre, H. Magnan, O. Heckmann, V. Briois, and D. Chandris, Phys. Rev. B **52**, 11 462 (1995).
- ¹⁸M. A. van Hove, R. J. Koestner, P. C. Stair, J. P. Biberian, L. L. Kesmodel, I. Bartos, and G. A. Somorjai, Surf. Sci. **103**, 189 (1981).
- ¹⁹N. Marsot, R. Belkhou, A. Barbier, N. Barrett, and C. Guillot (unpublished).
- ²⁰J. V. Barth, H. Brune, R. J. Behm, and G. Erth, Phys. Rev. B **42**, 9307 (1990).
- ²¹C. Brouder, J. Phys.: Condens. Matter **2**, 701 (1990).
- ²²P. Roubin, D. Chandris, G. Rossi, J. Lecante, M. C. Desjonqueres, and G. Treglia, Phys. Rev. Lett. **56**, 1272 (1986).
- ²³P. A. Lee and J. B. Pendry, Phys. Rev. B **11**, 2795 (1975).
- ²⁴W. Sucksmith and J. E. Thompson, Proc. R. Soc. London, Ser. A **225**, 362 (1954).
- ²⁵D. E. Sayers, E. A. Stern, and F. W. Lytle, Phys. Rev. Lett. **27**, 1204 (1971).
- ²⁶H. Lüth, *Surfaces and Interfaces of Solids* (Springer-Verlag, Berlin, 1993).
- ²⁷J. Thiele, R. Belkhou, H. Bulou, O. Heckmann, H. Magnan, P. Le Fèvre, D. Chandris, and C. Guillot, Surf. Sci. **384**, 120 (1997).
- ²⁸B. K. Teo and P. A. Lee, J. Am. Chem. Soc. **101**, 2815 (1979).
- ²⁹J. J. Rehr, J. Mustre de Leon, S. I. Zabinsky, and R. C. Albers, J. Am. Chem. Soc. **113**, 5135 (1991).
- ³⁰P. Grüter and U. T. Dürig, Phys. Rev. B **49**, 2021 (1994).
- ³¹S. T. Purcell, M. T. Johnson, N. W. E. Mc Gee, J. J. de Vries, W. B. Zeper, and W. Hoving, J. Appl. Phys. **73**, 1360 (1993).